AIAA JOURNAL
Vol. 41, No. 1, January 2003

Multilayered Piezoelectric Refined Plate Theory

Claire Ossadzow-David*
Université Paris VI, 75252 Paris Cedex 05, France
and
Maurice Touratier†
Ecole Nationale Supérieure des Arts et Métiers, 75013 Paris, France

A two-dimensional theory for the analysis of multilayered piezoelectric plates is presented. The theory is based on a hybrid approach in which the continuity conditions for both mechanical and electric unknowns at layer interfaces, as well as the imposed conditions on the bounding surfaces and at the interfaces, are independently satisfied. Then, the piezoelectric boundary-value problem is stated using mechanical displacements and electrostatic potential, in conjunction with the coupled piezoelectric constitutive law. The proposed model is simple to use, incorporating only five independent generalized displacements and one or two independent generalized electrostatic potentials as unknowns. The number of electric unknowns depends on the number of layers and electric prescribed conditions. The accuracy of the proposed theory is assessed through investigation of significant problems, for which an exact three-dimensional solution is known from Heyliger: first, in dynamics, the free vibrations of five-layered piezoelectric plates and second, in statics, for three-layered plates with an imposed force density. Results obtained with our model compare very well with the exact three-dimensional theory.

Nomenclature

A	=	lateral surface of the plate
a	=	length of the plate
$C_{kl}^{(i)}$	=	components of the elastic stiffness tensor of the ith layer
D_k	=	components of the electric displacement
E_l	=	components of the electric field
$e_{kl}^{(i)}$	=	components of the rotated piezoelectric tensor of the ith layer
h	=	total thickness of the plate
S_h	=	top surface of the plate
S_i	=	interface between the ith and $(i+1)$th layer
S_0	=	bottom surface of the plate
s_k	=	shear strains
V	=	space occupied by the plate
(x_1, x_2, z)	=	Cartesian coordinate system of the plate
z_i	=	distance between S_0 and S_i
$z_{i_{(0)}}$	=	distance between S_0 and the midsurface of the ith layer
δ	=	variational operator
$\varepsilon_{kl}^{(i)}$	=	components of the dielectric tensor of the ith layer
ε_0	=	permittivity of vacuum, $8.85 \cdot 10^{-12}$ F/m
ρ	=	mass density
φ	=	electrostatic potential
$\varphi^{iB}(x_\alpha, t)$	=	electrostatic potential on S_i
$\varphi^{iM}(x_\alpha, t)$	=	electrostatic potential on the midsurface of the ith layer
$\varphi^{iT}(x_\alpha, t)$	=	electrostatic potential on S_{i+1}
$\varphi^{N+1,B}(x_\alpha, t)$	=	electrostatic potential on S_h
$\varphi^{1B}(x_\alpha, t)$	=	electrostatic potential on S_0
$'$	=	derivation with respect to the thickness coordinate z
$\cdot$	=	differentiation with respect to time t

Received 23 February 2002; revision received 11 July 2002; accepted for publication 16 August 2002.

*Associate Professor, Laboratoire de Modélisation en Mécanique–Unité Mixte de Recherche Centre National de la Recherche Scientifique 7607, 4, Place Jussieu; david@lmm.jussieu.fr.

†Professor, Laboratoire de Mécanique des Systèmes et Procédés–Unité Mixte de Recherche Centre National de la Recherche Scientifique 8106, 151, Boulevard de l'Hôpital; Maurice.Touratier@paris.ensam.fr.

I. Introduction

THE development of so-called smart structures made of piezoelectric composites requires more and more precision in their design and sizing. The importance of efficient models has led to numerous theories. The first kind of approach is, in general, based on the hypothesis that the piezoelectric laminate will deform as a single uniform layer.

Application of the Kirchhoff–Love theory to piezoelectricity was developed by Tiersten,[1] Mindlin,[2] Lee and Moon,[3] and Lee.[4] However, accuracy is limited to thin plates. Chandrashekhara and Agawal[5] developed a first-order shear-deformation theory for single-layered plates. Extensions of the classical lamination plate theory to piezothermoelectricity were studied by Tauchert.[6] However, the electric fields generated by the stresses were not taken into account. Studies concerning specifically two-layered ceramic plates were developed by Vatal'yan et al.[7] Lee et al.[8] used series expansion about the thickness coordinate for the derivation of the two-dimensional equations of motion for uniform piezoelectric crystal plates. Yang and Yu[9] and Yong et al.[10] extended this theory to piezoelectric laminates. Uncoupled layerwise theories have then been developed.[11] Such models generally do not take into account the piezoelectric coupling in the equations of motion.

The second kind of approach takes this coupling into account. Hybrid theories, with a single-layer approach for the displacements and a layerwise modeling for the electrostatic potential, have been proposed. Mitchell and Reddy[12] used a third-order shear deformation theory for the displacements, while taking into account variations of the electrostatic potential through the thickness; Fernandes[13] and Fernandes and Pouget[14] proposed a piezoelectric laminate plate model accounting for transverse shear-effects refinements, as did Touratier.[15] Layerwise models were proposed, beginning with Pauley.[16] Pai et al.[17] proposed an induced-strain model for laminated piezoelectric plates. Heyliger[18] and Heyliger and Brooks[19] developed an exact three-dimensional solution for laminated piezoelectric plates. However, approximate piezoelectric plate models do not simultaneously take into account the continuity and imposed conditions on mechanical and electric quantities. Asymptotic theories, taking into account the continuity conditions on the mechanical and electrical quantities exist, but only concern thin structures.[20]

We propose here a new bidimensional theory for the modeling of multilayered piezoelectric plates. It extends previous works on

plates and shells[21,22] to piezoelectricity by combining the previous equivalent single-layer approach for the displacement field with quadratic variations of the electrostatic potential through each piezoelectric layer. The electrostatic potential is automatically continued at layer interfaces by a quadratic layer-wise description in the thickness direction. In addition, transverse shear stresses, as well as the electric displacement, are independently continued, using uncoupled constitutive law for those two fields at the first stage. Refinements of the transverse shear and membrane terms are taken into account, in the displacement field, by means of trigonometric functions. Moreover, we allow values for the electrostatic potential to be imposed either on the top and bottom surfaces of the structure, or at layer interfaces. Finally, the piezoelectric boundary-value problem is constructed using the consistant coupled constitutive law, in conjunction with the displacements and electrostatic potential fields. The proposed piezoelectric plate model is evaluated for significant problems, for which the exact three-dimensional solution is known.[19]

II. Piezoelectric Plate Model

A. Introduction to Plate Theory

We consider an undeformed laminated plate of constant thickness, consisting of an arrangement of a finite number N of piezoelectric layers (Fig. 1). The reference surface coincides with the bottom surface of the plate S_0. In this paper, the Einsteinian summation convention applies to repeated indices, where Latin indices range from 1 to 3 and Greek indices range from 1 to 2.

B. Displacement Field

Geometrical linear plates are considered, including an elastic-linear behavior for laminates. The transverse normal stress is ignored, and it is assumed that no tangential tractions are exerted on the upper and lower surfaces of the plate.

The components of the displacement field of any point $M(x_1, x_2, z)$ of the volume occupied by the plate are assumed in the following form:

$$\begin{aligned} U_\alpha(x_1,x_2,z,t) &= u_\alpha(x_1,x_2,t) + z\eta_\alpha(x_1,x_2,t) \\ &\quad + f(z)\psi_\alpha(x_1,x_2,t) + g(z)\gamma_\alpha^0(x_1,x_2,t) \\ &\quad + \sum_{m=1}^{N-1} u_{(m)_\alpha}(x_1,x_2,t)(z-z_m)H(z-z_m) \\ U_3(x_1,x_2,z,t) &= w(x_1,x_2,t) \end{aligned} \tag{1}$$

where [as suggested by Touratier[23] for $f(z)$]

$$f(z) = (h/\pi)\sin(\pi z/h), \qquad g(z) = (h/\pi)\cos(\pi z/h) \tag{2}$$

H is the Heaviside step function defined by

$$H(z-z_m) = \begin{cases} 1 & \text{for} \quad z \geq z_m \\ 0 & \text{for} \quad z < z_m \end{cases} \tag{3}$$

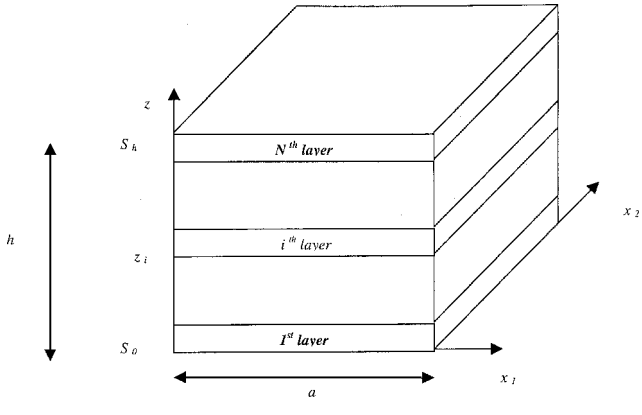

Fig. 1 Multilayered piezoelectric plate.

This step function has been previously used by Di Sciuva[24] and He,[25] among others. As in Ref. 23, the choice for $f(z)$ can be justified in a discrete-layer approach from the three-dimensional works of Cheng[26] for thick plates.

In this displacement field, u_α are the membrane displacements, γ_α^0 are the transverse shear strains at $z=0$, and w is the transverse deflection of the shell. Here, η_α and ψ_α are functions to be determined using the conditions for the transverse shear stresses on the top and bottom surfaces of the plate. With the help of $u_{(m)_\alpha}$, which represent the generalized displacements per layer, the continuity of the displacements at layer interfaces are automatically satisfied from the Heaviside function. They are determined from the continuity conditions on the transverse shear stresses at the interfaces. The transverse shear stresses per layer are given by the classic uncoupled orthotropic constitutive law:

$$\sigma_{6-\alpha}^{(i)\text{uncoupled}} = C_{6-\alpha,6-\alpha}^{(i)} s_{6-\alpha}, \qquad i = 1,\ldots,N-1, \qquad \alpha = 1,2 \tag{4}$$

To reduce the number of unknowns in the displacement field, the conditions on the top and bottom surfaces and the continuity conditions of transverse shear stresses at layer interfaces are exploited, using the purely elastic constitutive law, without any coupling with electric quantities at this stage. This allows the elimination of η_α and ψ_α:

$$\eta_\alpha = -\frac{1}{2}\sum_{m=1}^{N-1} u_{(m)_\alpha} - w_{,\alpha}, \qquad \psi_\alpha = \frac{1}{2}\sum_{m=1}^{N-1} u_{(m)_\alpha} \tag{5}$$

The continuity conditions for transverse shear stresses lead to the following system of $2(N-1)$ equations with the $2(N-1)$ unknowns $u_{(m)_\alpha}$:

$$\begin{aligned} &C_{6-\alpha,6-\alpha}^{(i)}\left[g'(z_i)\gamma_\alpha^0 + \sum_{m=1}^{i-1}\frac{1}{2}\{f'(z_i)-1\}u_{(m)_\alpha}\right] \\ &\quad = C_{6-\alpha,6-\alpha}^{(i+1)}\left[g'(z_i)\gamma_\alpha^0 + \sum_{m=1}^{i}\frac{1}{2}\{f'(z_i)-1\}u_{(m)_\alpha}\right] \\ &\qquad i = 1,\ldots,N-1, \qquad \alpha = 1,2 \end{aligned} \tag{6}$$

where primes denote derivation with respect to the thickness coordinate z. Those latter functions can then be expressed in terms of the γ_α^0:

$$u_{(m)_\alpha} = \lambda_{(m)_\alpha}\gamma_\alpha^0 \text{ (no summation)} \tag{7}$$

where the $\lambda_{(m)_\alpha}$ are given by solving system (6).

The final form of the displacement field is given by

$$U_\alpha = u_\alpha - zw_{,\alpha} + h_\alpha\gamma_\alpha^0, \qquad U_3 = w \tag{8}$$

where h_α are functions of the global thickness coordinate z:

$$h_\alpha(z) = g(z) + \sum_{m=1}^{N}\left[\frac{1}{2}[f(z)-z] + (z-z_m)H(z-z_m)\right]\lambda_{(m)_\alpha} \tag{9}$$

This kinematic field was developed by Ossadzow et al.[21,22]

C. Electrostatic Potential

To approximate the electrostatic potential, we consider the purely electric state of the plate, as was done for elasticity, to write interface conditions and conditions at the top and bottom surfaces of the plate. Then, when formulating the boundary piezoelectric boundary-value problem, we will include coupled electromechanical constitutive laws.

The electrostatic potential φ is approximated in the following form:

$$\varphi(x_1,x_2,z,t) = \sum_{i=1}^{n}\varphi^i(x_1,x_2,z,t)\chi^i(z) \tag{10}$$

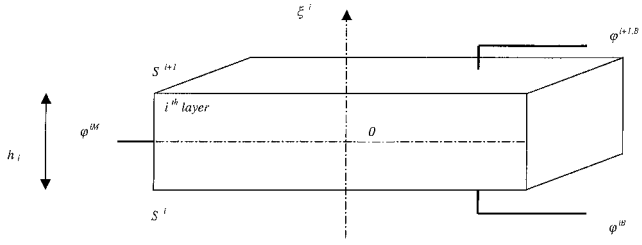

Fig. 2 Configuration of the *i*th layer.

where the φ^i are the potentials, per layer, and χ^i is the characteristic ith-layer function,

$$\chi^i(z) = \begin{cases} 1 & \text{if} \quad z \in [z^i, z^{i+1}[\\ 0 & \text{if} \quad z \notin [z^i, z^{i+1}[\end{cases} \tag{11}$$

When the thickness coordinate ξ^i is introduced (Fig. 2) for each layer,

$$-1 \le \xi^i \le 1, \qquad \xi^i = 2\big(z - z_{i_{(0)}}\big)\big/h^i \tag{12}$$

the φ^i are taken as

$$\varphi^i(x_j, t) = \tfrac{1}{2}\xi^i(\xi^i - 1)\varphi^{iB}(x_\alpha, t) + [1 - (\xi^i)^2]\varphi^{iM}(x_\alpha, t) + \tfrac{1}{2}\xi^i(\xi^i + 1)\varphi^{iT}(x_\alpha, t) \qquad (i = 1, \ldots, N) \tag{13}$$

Thus,

$$\varphi^i(x_\alpha, z_i, t) = \varphi^{iB}(x_\alpha, t), \qquad \varphi^i(x_\alpha, z_{i+1}, t) = \varphi^{iT}(x_\alpha, t)$$
$$\varphi^i[x_\alpha, (z_{i+1} - z_i)/2, t] = \varphi^{iM}(x_\alpha, t) \qquad (i = 1, \ldots, N) \tag{14}$$

Because

$$\varphi^{i+1,B}(x_\alpha, z_i, t) = \varphi^{iT}(x_\alpha, z_i, t) \qquad (i = 0, \ldots, N) \tag{15}$$

note that the continuity of the electrostatic potential at the layer interfaces is automatically satisfied, as can be seen in Fig. 2.

Starting from the first layer, we choose to keep $\varphi^{iB}(x_\alpha, t)$ and $\varphi^{iM}(x_\alpha, t)$ as unknowns. The φ^i can then be written as

$$\varphi^i(x_j, t) = \tfrac{1}{2}\xi^i(\xi^i - 1)\varphi^{iB}(x_\alpha, t) + [1 - (\xi^i)^2]\varphi^{iM}(x_\alpha, t) + \tfrac{1}{2}\xi^i(\xi^i + 1)\varphi^{i+1,B}(x_\alpha, t) \qquad (i = 1, \ldots, N) \tag{16}$$

For future applications, we suppose that p values for the electrostatic potential are given, which means that p values for the $\varphi^{iB}(x_\alpha, t)$ are imposed, depending on the kind of prescribed electric conditions. These values can be given on the top and bottom surfaces of the plate, or at layer interfaces.

The uncoupled piezoelectric constitutive law gives

$$D_3^{\text{uncoupled}} = \varepsilon_{33}E_3 = -\varepsilon_{33}\varphi_{,3} \tag{17}$$

The continuity of the purely electric displacement D_3 at layer interfaces and the conditions on top and bottom surfaces and at the p layer interfaces lead to a system of $N + p - 1$ equations which allow the elimination of part of the φ^{iB} and φ^{iM}, as will be seen in the examples developed in Secs. III and IV. The φ^{iB} that are chosen to remain unknown will be denoted $\{\varphi^{i_1 B}, \ldots, \varphi^{i_n B}\}$. The φ^{jM} that are chosen to remain unknown will be denoted $\{\varphi^{j_1 M}, \ldots, \varphi^{j_m M}\}$. Note that

$$i_n + j_m = 2N + 1 - (N + p - 1) = N - p + 2 \tag{18}$$

(There are $2N + 1$ unknowns at the beginning and $N + p - 1$ conditions.) The electrostatic potential can then be written in the following form:

$$\varphi = \sum_{i=i_1}^{i_n} Q^{iB}\varphi^{iB} + \sum_{j=j_1}^{j_m} Q^{jM}\varphi^{jM} \tag{19}$$

where the Q^{iB} and Q^{jM} are polynomial functions of the global thickness coordinate z (examples in Sec. III), coming from the imposed conditions for the potential, as described before.

Now note that the coupled piezoelectric constitutive law gives

$$D_3^{\text{coupled}} = \varepsilon_{33}E_3 + e_{3j}s_j \tag{20}$$

The $\varepsilon_{33}E_3$ term is very small compared to the $e_{3j}s_j$ terms; thus, after solving any boundary value problem as will be explained in Sec. II.E, the final (coupled) electric displacement will be corrected in the postprocessing phase as

$$\tilde{D}_3^{\text{coupled}} = \varepsilon_{33}E_3 + e_{3j}s_j - \big[e_{3j}^{(k)}s_j^{(k)}(z_k)\chi^k(z) - e_{3j}^{(k+1)}s_j^{(k+1)}(z_k)\chi^{k+1}(z)\big] \tag{21}$$

where the (k) exponent characterizes the quantities related to the kth layer and the $(k + 1)$ exponent the quantities related to the $(k + 1)$th layer.

For convenience, we will denote by $\tilde{D}^{\text{coupled}}$ the final (coupled) electric displacement field. (Only its third component is corrected of course.) Therefore, at the kth layer interface, the continuity of the modified coupled electric displacement $\tilde{D}_3^{\text{coupled}}$ is satisfied [$\varepsilon_{33}E_3$ being continuous, from Eqs. (17–20)] because we have

$$\lim_{z \to z_k, z < z_k} \tilde{D}_3^{\text{coupled}} = \lim_{z \to z_k, z < z_k} \Big\{\varepsilon_{33}E_3 + \underbrace{e_{3j}s_j - e_{3j}^{(k)}s_j^{(k)}(z_k)}_{0}\Big\}$$
$$= \lim_{z \to z_k}\{\varepsilon_{33}E_3\} = \lim_{z \to z_k, z > z_k} \Big\{\varepsilon_{33}E_3 + \underbrace{e_{3j}s_j - e_{3j}^{(k+1)}s_j^{(k+1)}(z_k)}_{0}\Big\} \tag{22}$$

Hereafter, depending on the kind of prescribed electric conditions, we will show how to build the potential field because our method is new, as it is possible to check, and different from a usual layerwise method, which does not exploit all of the imposed conditions. It allows to reduce the size of any boundary-value problem.

D. Linear-Piezoelectric Constitutive Law

The constitutive law of a piezoelectric material adopted in our model is from Tiersten[1] and is expressed by

$$\sigma_i^{\text{coupled}} = C_{ij}s_j - e_{ki}E_k, \qquad D_k^{\text{coupled}} = \varepsilon_{kl}E_l + e_{ki}s_i \tag{23}$$

The standard contracted notation, with $i, j = 1, \ldots, 6$, and $k, l = 1, \ldots, 3$, has been used in these equations. The poling direction is coincident with the z axis.

When the results stated in Sec. II.C are used, the electric field is related to the electrostatic potential φ through the relation

$$\boldsymbol{E} = -\text{grad}\,\varphi = -\sum_{i=i_1}^{i_n} \text{grad}[Q^{iB}\ \varphi^{iB}] - \sum_{j=j_1}^{j_m} \text{grad}[Q^{jM}\ \varphi^{jM}] \tag{24}$$

For the materials used in this study, we assume that the nonzero components of the rotated piezoelectric tensor e_{ki}, the elastic stiffness tensor C_{ij}, and the components of the dielectric tensor ε_{kl} are those of orthorhombic crystal. The nonzero elements of those two latter tensors will be taken as e_{31}, e_{32}, e_{33}, e_{24}, and e_{15}, and ε_{11}, ε_{22}, and ε_{33}.

When a zero value of the transverse normal stress is taken into account, as usual for plates, the constitutive law per layer can be written as follows:

$$\sigma_i^{\text{coupled}} = C_{ij}^{2D}s_j - e_{ki}^{2D}E_k, \qquad D_k^{\text{coupled}} = \varepsilon_{kl}^{2D}E_l + e_{kj}^{2D}s_j \tag{25}$$

where

$$C_{ij}^{2D} = C_{ij} - C_{i3}(C_{3j}/C_{33}), \qquad e_{ki}^{2D} = e_{ki} - C_{i3}(e_{k3}/C_{33})$$
$$\varepsilon_{kl}^{2D} = \varepsilon_{kl} + e_{k3}(e_{l3}/C_{33}) \tag{26}$$

E. Two-Dimensional Boundary-Value Problem

The equations of motion and the natural boundary conditions are derived via Hamilton's principle:

$$\int_0^t \left\{ \int_V^{\sigma^{i\,\text{coupled}}} \delta s_i \, \mathrm{d}V + \int_V D_i^{\text{coupled}} \delta\varphi_{,i} \, \mathrm{d}V + \int_V \boldsymbol{f}_v \cdot \delta \boldsymbol{U} \, \mathrm{d}V + \int_A \boldsymbol{f}_s \cdot \delta \boldsymbol{U} \, \mathrm{d}A + \int_{S_0} (-p_h + p_0) \, \mathrm{d}S + \int_S W \delta\varphi \, \mathrm{d}V \right\} \times \mathrm{d}t = 0 \tag{27}$$

where f_v^i are components of body forces, f_s^i the prescribed components of the load on the undeformed lateral surface of the plate, and p_0 and p_h the prescribed components of traction on the surfaces S_0 and S_h. W is the density of electric forces.

When integration is performed through the thickness of the plate, the following equations of motion are deduced from Eqs. (8), (23), (24), and (27):

$$\begin{gathered} N^{\alpha}_{(1),\alpha} + N^{\alpha\beta}_{(2),\beta} = I_1 \ddot{u}_\alpha - I_2 \ddot{w}_{,\alpha} + I_3^{\alpha} \ddot{\gamma}_\alpha^0 \\ M^{\alpha}_{(1),\alpha\alpha} + M^{\alpha\beta}_{(2),\alpha\beta} = I_2 \ddot{u}_{\alpha,\alpha} - I_4 \ddot{w}_{,\alpha\alpha} + I_5^{\alpha} \ddot{\gamma}^0_{\alpha,\alpha} + I_1 \ddot{w} \\ N^{\alpha}_{(3),\alpha} + N^{\alpha\beta}_{(4),\beta} + N^{\alpha}_{(5)} = I_3^{\alpha} \ddot{u}_\alpha - I_5^{\alpha} \ddot{w}_{,\alpha} + I_6^{\alpha} \ddot{\gamma}_\alpha^0 \\ \mathcal{N}^{iB} + \mathcal{M}^{iB\alpha}_{,\alpha} = 0, \qquad i \in \{i_1, \ldots, i_n\} \\ \mathcal{N}^{jM} + \mathcal{M}^{jM\alpha}_{,\alpha} = 0, \qquad j \in \{j_1, \ldots, j_m\} \qquad (\alpha = 1, 2) \end{gathered} \tag{28}$$

where an overdot is used for differentiation to time t.

In the last expression, the generalized stresses are given by

$$N^{\alpha}_{(1)} = -\int_0^h \{C_{\alpha j} s_j - e_{3\alpha} E_3\} \, \mathrm{d}z, \qquad N^{\alpha\beta}_{(2)} = -\int_0^h C_{66} s_6 \Delta_{\alpha\beta} \, \mathrm{d}z$$

$$N^{(3)^{\alpha}} = -\int_0^h \{C_{\alpha j} s_j - e_{3\alpha} E_3\} h_\alpha \, \mathrm{d}z$$

$$N^{\alpha\beta}_{(4)} = -\int_0^h C_{66} s_6 \Delta_{\alpha\beta} h_\alpha \, \mathrm{d}z$$

$$N^{\alpha}_{(5)} = \int_0^h \frac{1}{2} \{C_{6-\alpha,6-\alpha} s_{6-\alpha} - e_{2,6-\alpha} E_2\} h_{\alpha,3} \, \mathrm{d}z$$

$$M^{\alpha}_{(1)} = -\int_0^h \{C_{\alpha j} s_j - e_{3\alpha} E_3\} z \, \mathrm{d}z, \qquad M^{\alpha\beta}_{(2)} = -\int_0^h C_{66} s_6 \Delta_{\alpha\beta} z \, \mathrm{d}z$$

$$\mathcal{N}^{iB} = \int_0^h E_3 \varepsilon_{33} Q^{iB'} \, \mathrm{d}z, \qquad i \in \{i_1, \ldots, i_n\}$$

$$\mathcal{N}^{jM} = \int_0^h E_3 \varepsilon_{33} Q^{jM'} \, \mathrm{d}z, \qquad j \in \{j_1, \ldots, j_m\}$$

$$\mathcal{M}^{iB^{\alpha}} = -\int_0^h \{E_\alpha \varepsilon_{\alpha\alpha} + e_{k\alpha} s_{\alpha,\alpha}\} Q^{iB} \, \mathrm{d}z, \qquad i \in \{i_1, \ldots, i_n\}$$

$$\mathcal{M}^{iM^{\alpha}} = -\int_0^h \{E_\alpha \varepsilon_{\alpha\alpha} + e_{k\alpha} s_{\alpha,\alpha}\} Q^{iM} \, \mathrm{d}z, \qquad j \in \{j_1, \ldots, j_m\} \tag{29}$$

where

$$\Delta_{\alpha\beta} = \begin{cases} 1 & \text{if} \quad \alpha \neq \beta \\ 0 & \text{if} \quad \alpha = \beta \end{cases}$$

and primes denote derivation with respect to the thickness coordinate z.

The generalized external mechanical forces are given by

$$F^1_{v\alpha} = \int_0^h f_{v\alpha} \, \mathrm{d}z, \qquad F^2_{v\alpha} = -\int_0^h f_{v\alpha} Z \, \mathrm{d}z$$

$$F^3_{v\alpha} = \int_0^h f_{v\alpha} h_\alpha \, \mathrm{d}z, \qquad F^3_v = \int_0^h f_{v_3} \, \mathrm{d}z, \qquad P = -p_h + p_0 \tag{30}$$

The generalized external electrostatic forces are given by

$$W^{iB} = \int_0^h W Q^{iB} \, \mathrm{d}z, \qquad i \in \{i_1, \ldots, i_n\}$$

$$W^{jM} = \int_0^h W Q^{jM} \, \mathrm{d}z, \qquad j \in \{j_1, \ldots, j_m\} \tag{31}$$

The inertia terms are given by

$$I_1 = \int_0^h \rho \, \mathrm{d}z, \qquad I_2 = \int_0^h \rho z \, \mathrm{d}z, \qquad I_3^{(\alpha)} = \int_0^h \rho h_\alpha(z) \, \mathrm{d}z$$

$$I_4 = \int_0^h \rho z^2 \, \mathrm{d}z, \qquad I_5^{(\alpha)} = \int_0^h \rho z h_\alpha(z) \, \mathrm{d}z$$

$$I_6^{(\alpha)} = \int_0^h \rho z h_\alpha^2(z) \, \mathrm{d}z \tag{32}$$

The boundary conditions leading to a regular problem are

$$\begin{gathered} \left[N^{(1)^{\alpha}} n_\alpha + N^{(2)^{\alpha\beta}} n_\beta\right] = F^1_{v\alpha} \qquad \text{or} \qquad \delta u_\alpha = 0 \\ \left\lfloor M^{(1)^{\alpha}}, \alpha + M^{(2)^{\alpha\beta}}, \beta \right\rfloor = F^2_{v\alpha}, \qquad \text{or} \qquad \delta w = 0 \\ N^{(4)^{\alpha\beta}} n_\beta = F^3_{v\alpha} \qquad \text{or} \qquad \delta\gamma^0_\alpha = 0 \\ \left\lfloor M^{(1)^{\alpha}} n_\alpha + M^{(2)^{\alpha\beta_{n_\beta}}} \right\rfloor = F_{v_3} \qquad \text{or} \qquad \delta w_{,\alpha} = 0 \\ \mathcal{M}^{iB^{\alpha}} n_\alpha = W^{iB} \qquad \text{or} \qquad \delta\varphi^{iB} = 0, \qquad i \in \{i_1, \ldots, i_n\} \\ \mathcal{M}^{jM^{\alpha}} n_\alpha = W^{jM} \qquad \text{or} \qquad \delta\varphi^{jM} = 0, \qquad j \in \{j_1, \ldots, j_m\} \end{gathered} \tag{33}$$

The equations of motion are deduced from Eqs. (28), including the constitutive law given by Eqs. (23–26), (8), and (19), and, of course, using Eqs. (29).

III. Evaluations of the Piezoelectric Plate Model

To assess the accuracy of the present theory, we have studied problems for which an exact three-dimensional elasticity solution is known[18,19]: In statics, our model is evaluated on a three-layered cross ply made of polyvinylidene fluoride (PVDF) and in dynamics through free vibrations of a five-layered piezoelectric plate. Then, we have applied our model to a significative example.

The piezoelectric and dielectric coefficients being very small compared to the elastic constants, we introduce nondimensional quantities

$$\begin{gathered} C_{ij}^{2D^*} = C_{ij}^{2D} \big/ C_0, \qquad e_{ki}^{2D^*} = E_0 \left(e_{ki}^{2D} \big/ C_0\right) \\ \varepsilon_{kl}^{2D^*} = E_0^2 \left(\varepsilon_{kl}^{2D} \big/ C_0\right) \end{gathered} \tag{34}$$

where

$$C_0 = C_{11}^1, \qquad E_0 = 10^{10} \ \text{V/m} \tag{35}$$

Then the generalized displacements and potentials are written as follows:

$$\begin{aligned} &\left(\bar{u}_\alpha, \bar{w}, \bar{\gamma}^0_\alpha, \bar{\varphi}^{iB}, \bar{\varphi}^{jM}\right) \\ &\quad = \left[C_0 u_\alpha, C_0 w, C_0 \gamma^0_\alpha, \left(C_0 \varphi^{iB} \big/ E_0\right), \left(C_0 \varphi^{jM} \big/ E_0\right)\right] \end{aligned} \tag{36}$$

The same unit mass density will be used for all materials.

A. Application of the Piezoelectric Plate Model to Dynamics

For this example, we consider a square, simply supported five-layered piezoelectric plate, in closed circuit, where $\varphi = 0$ at the top

Table 1 Elastic, piezoelectric and dielectric properties of PZT4, PVDF, and epoxy

Moduli	PZT4	PVDF	Epoxy
C_{1111}, Gpa	139	238.24	134.86
C_{2222}, Gpa	139	23.6	14.352
C_{3333}, Gpa	115	10.64	14.352
C_{1122}, Gpa	77.8	3.98	5.1563
C_{1133}, Gpa	74.3	2.19	5.1563
C_{2233}, Gpa	74.3	1.92	7.1329
C_{2323}, Gpa	25.6	2.15	3.606
C_{1313}, Gpa	25.6	4.4	5.654
C_{1212}, Gpa	30.6	6.43	5.654
e_{31}, C/m^2	−5.2	−0.13	0
e_{32}, C/m^2	−5.2	−0.145	0
e_{33}, C/m^2	15.1	−0.276	0
e_{24}, C/m^2	12.7	−0.009	0
$\varepsilon_{11}/\varepsilon_0$	1475	12.5	3.5
$\varepsilon_{22}/\varepsilon_0$	1475	11.98	3.0
$\varepsilon_{33}/\varepsilon_0$	1300	11.98	3.0

and bottom surfaces of the plates. From Eq. (8), the simple support conditions for a square plate of length a are simulated by

$$\begin{aligned} u_1(x_1,0,z,t) &= u_1(x_1,a,z,t) = 0 \\ u_2(0,x_2,z,t) &= u_2(a,x_2,z,t) = 0 \\ w(x_1,0,z,t) &= w(x_1,a,z,t) = 0 \\ w(0,x_2,z,t) &= w(a,x_2,z,t) = 0 \\ \gamma_1^0(x_1,0,z,t) &= \gamma_1^0(x_1,a,z,t) = 0 \\ \gamma_2^0(0,x_2,z,t) &= \gamma_2^0(a,x_2,z,t) = 0 \end{aligned} \tag{37}$$

The height of the plate is fixed at $h = 0.01$ m .

The external layers are made of plumbum zirconate titanate (PZT)4, the three internal ones being a symmetric elastic epoxy 0/90/0 cross-ply. See Table 1 for all of the piezoelectric properties of those materials. The same unit mass density will be used for all materials.

The piezoelectric coefficients of the three internal layers are identical. For the dielectric coefficients, the three elastic layers have the same ε_{33}. The ε_{11} and ε_{22} are very close. Therefore, we consider that those three layers behave as a single layer, from the electric point of view. The five-layered plate will, thus, be modeled as a three-layered elastic one, its core being the elastic-epoxy cross ply.

From Eqs. (10) and (13), the approximation of the electrostatic potential thus becomes

$$\begin{aligned} \varphi(x_j,t) = {} & \left\{ \tfrac{1}{2}\xi^1(\xi^1-1)\varphi^{1B}(x_\alpha,t) + [1-(\xi^1)^2]\varphi^{1M}(x_\alpha,t) \right. \\ & \left. + \tfrac{1}{2}\xi^1(\xi^1+1)\varphi^{2B}(x_\alpha,t) \right\}\chi^1 + \left\{ \tfrac{1}{2}\xi^2(\xi^2-1)\varphi^{2B}(x_\alpha,t) \right. \\ & \left. + [1-(\xi^2)^2]\varphi^{2M}(x_\alpha,t) + \tfrac{1}{2}\xi^2(\xi^2+1)\varphi^{3B}(x_\alpha,t) \right\}\chi^2 \\ & + \left\{ \tfrac{1}{2}\xi^3(\xi^3-1)\varphi^{3B}(x_\alpha,t) + [1-(\xi^3)^2]\varphi^{3M}(x_\alpha,t) \right. \\ & \left. + \tfrac{1}{2}\xi^3(\xi^3+1)\varphi^{4B}(x_\alpha,t) \right\}\chi^3 \end{aligned} \tag{38}$$

The plate is in closed circuit:

$$\varphi^{1B}(x_\alpha,t) = \varphi^{4B}(x_\alpha,t) = 0 \tag{39}$$

Moreover, the symmetry allows

$$\varphi^{2B}(x_\alpha,t) = \varphi^{3B}(x_\alpha,t), \qquad \varphi^{1M}(x_\alpha,t) = \varphi^{3M}(x_\alpha,t) \tag{40}$$

to be imposed. This results in

$$\begin{aligned} \varphi(x_j,t) = {} & \left\{ [1-(\xi^1)^2]\varphi^{1M}(x_\alpha,t) + \tfrac{1}{2}\xi^1(\xi^1+1)\varphi^{2B}(x_\alpha,t) \right\}\chi^1 \\ & + \left\{ \tfrac{1}{2}\xi^2(\xi^2-1)\varphi^{2B}(x_\alpha,t) + [1-(\xi^2)^2]\varphi^{2M}(x_\alpha,t) \right. \\ & \left. + \tfrac{1}{2}\xi^2(\xi^2+1)\varphi^{2B}(x_\alpha,t) \right\}\chi^2 + \left\{ \tfrac{1}{2}\xi^3(\xi^3-1)\varphi^{2B}(x_\alpha,t) \right. \\ & \left. + [1-(\xi^3)^2]\varphi^{1M}(x_\alpha,t) \right\}\chi^3 \end{aligned} \tag{41}$$

Because of the symmetries, the continuity of the uncoupled electric displacement D_3 at layer interfaces is written at the first interface as

$$-\varepsilon_{33}^1\varphi_{,3}^1(x_\alpha,z_1,t) = -\varepsilon_{33}^2\varphi_{,3}^2(x_\alpha,z_1,t) \tag{42}$$

This leads to an equation that allows φ^{2B} to be expressed in terms of φ^{1M} and φ^{2M},

$$\varphi^{2B}(x_\alpha,t) = \lambda^{2B,1M}\varphi^{1M}(x_\alpha,t) + \lambda^{2B,2M}\varphi^{2M}(x_\alpha,t) \tag{43}$$

The electrostatic potential can then be written in the following form:

$$\varphi(x_j,t) = Q^{1M}(z)\varphi^{1M}(x_\alpha,t) + Q^{2M}(z)\varphi^{2M}(x_\alpha,t) \tag{44}$$

where

$$\begin{aligned} Q_{(z)}^{1M} = {} & \left\{ [1-(\xi^1)^2] + \tfrac{1}{2}\xi^1(\xi^1+1)\lambda^{2B,1M} \right\}\chi^1 \\ & + \left[\tfrac{1}{2}\xi^2(\xi^2-1)\lambda^{2B,1M} + \tfrac{1}{2}\xi^2(\xi^2+1)\lambda^{2B,1M} \right]\chi^2 \\ & + \left\{ [1-(\xi^3)^2] + \tfrac{1}{2}\xi^3(\xi^3-1)\lambda^{2B,1M} \right\}\chi^3 \\ Q_{(z)}^{2M} = {} & \left[\tfrac{1}{2}\xi^1(\xi^1+1)\lambda^{2B,2M} \right]\chi^1 + \left\{ \tfrac{1}{2}\xi^2(\xi^2-1)\lambda^{2B,2M} \right. \\ & \left. + [1-(\xi^2)^2] + \tfrac{1}{2}\xi^2(\xi^2+1)\lambda^{2B,2M} \right\}\chi^2 \\ & + \left[\tfrac{1}{2}\xi^3(\xi^3-1)\lambda^{2B,2M} \right]\chi^3 \end{aligned} \tag{45}$$

The mechanical generalized displacements remaining unknowns are u_α, w, and γ_α^0. The electrical generalized unknowns are φ^{1M} and φ^{2M}. The solution of Eqs. (28–33), including Eqs. (8), (25), and (44), in terms of the generalized unkowns given by Eq. (36), is sought under the form

$$\begin{aligned} \bar{u}_1(x_\alpha,t) &= A_1 e^{j\omega t}\cos p_1x_1 \sin p_2x_2 \\ \bar{u}_2(x_\alpha,t) &= A_2 e^{j\omega t}\sin p_1x_1 \cos p_2x_2 \\ \bar{w}(x_\alpha,t) &= B e^{j\omega t}\sin p_1x_1 \sin p_2x_2 \\ \bar{\gamma}_1^0(x_\alpha,t) &= C_1 e^{j\omega t}\cos p_1x_1 \sin p_2x_2 \\ \bar{\gamma}_2^0(x_\alpha,t) &= C_2 e^{j\omega t}\sin p_1x_1 \cos p_2x_2 \end{aligned} \tag{46}$$

$$\begin{aligned} \bar{\varphi}^{1M}(x_\alpha,t) &= \Phi_1 e^{j\omega t}\sin p_1x_1 \sin p_2x_2 \\ \bar{\varphi}^{2M}(x_\alpha,t) &= \Phi_2 e^{j\omega t}\sin p_1x_1 \sin p_2x_2 \end{aligned} \tag{47}$$

where

$$p_1 = p_2 = \pi/a \tag{48}$$

which characterizes the propagation of harmonic plane waves. The boundary conditions given by Eq. (37) for a simply supported plate are satisfied. Substituting the expressions (46) and (47) into the equations of motion given by Eqs. (28) with Eqs. (29–33) and (8), (25), and (44), for free motions, seven linear equations in terms of A_1, A_2, B, C_1, C_2, Φ_1, and Φ_2 are obtained. For a nontrivial solution, the determinant of the matrix of coefficients A_1, A_2, B, C_1, C_2, Φ_1, and Φ_2 must vanish, resulting in the following frequency equation:

$$\det[K^1 - \omega^2 M] = 0 \tag{49}$$

The coefficients of the corresponding stiffness matrix K^1 and mass matrix M are given in Appendix A. The frequencies corresponding to the two first thickness modes are shown in Table 2. They can be compared to those of the exact solution of Heyliger.[18] The through-the-thickness distributions of normalized electrostatic potential $\bar{\varphi}$, electric displacement $\bar{D}_3$, shear-stress $\bar{\sigma}_{13}$, and normal in-plane stress $\bar{\sigma}_{11}$ are shown in Figs. 3–6 for $a/h = 4$. These normalized quantities are computed from Eqs. (47) and (48), where

Table 2 Frequency parameters for the five-layered piezoelectric plate

	$\gamma = \omega/100$	
a/h	Model	Exact solution
4	194,903	191,301
	251,763	250,769
50	15,592.3	15,681
	209,479	209,704

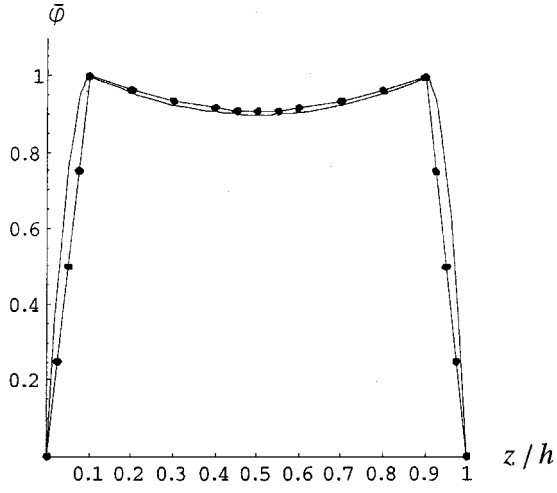

Fig. 3 Thickness distribution of the normalized electrostatic potential, first mode, five-layered plate, $a/h = 4$: ——, model and ●, exact solution.

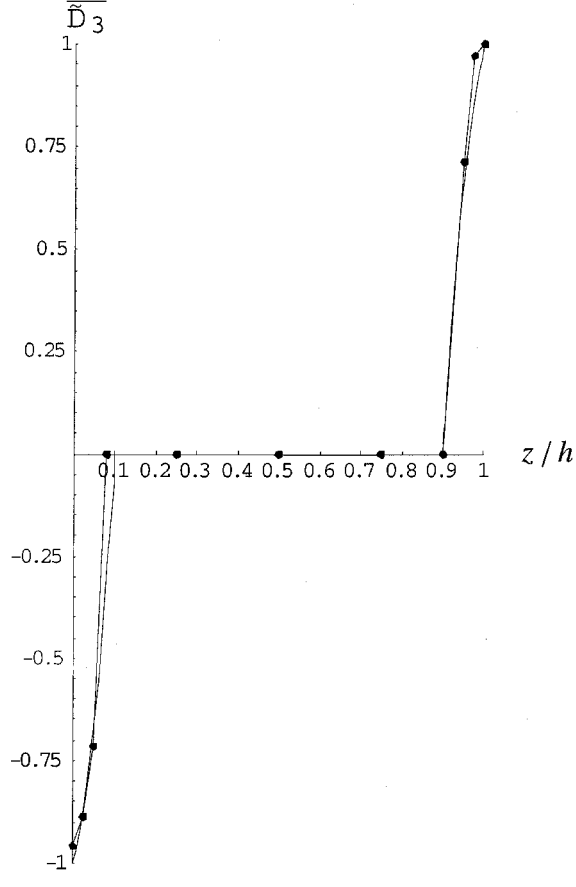

Fig. 4 Thickness distribution of the normalized electric displacement $\bar{\tilde{D}}_3$ five-layered plate, $a/h = 4$: ——, model and ●, exact solution.

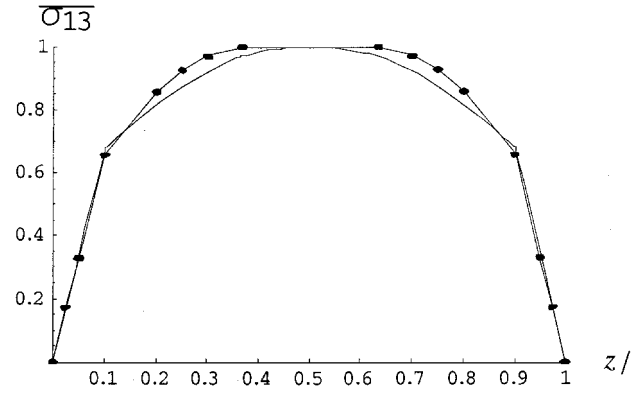

Fig. 5 Thickness distribution of the normalized shear-stress $\bar{\sigma}_{13}$, five-layered plate, $a/h = 4$: ——, model and ●, exact solution.

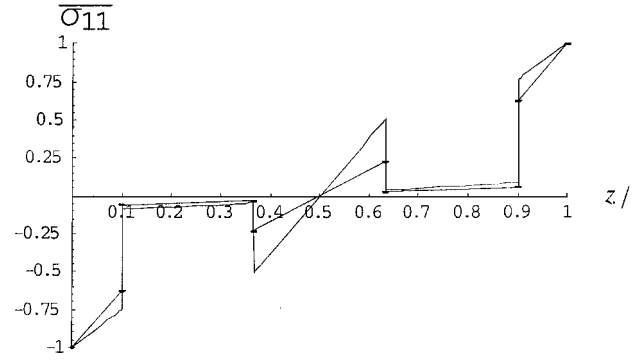

Fig. 6 Thickness distribution of the normalized in-plane stress $\bar{\sigma}_{11}$, five-layered plate, $a/h = 4$: ——, model and ●, exact solution.

we recall that the electric displacement is computed according to

$$D_3 = \varepsilon_{33} E_3 + e_{3j} s_j - e_{3j} s_j(z_k) \tag{50}$$

$$\bar{\varphi}(z) = \frac{\bar{\varphi}(a/2, a/2, z)}{\varphi(a/2, a/2, h/2)}, \qquad \bar{D}_3(z) = \frac{D_3(0, a/2, z)}{D_3(0, a/2, h)} \tag{51}$$

$$\bar{\sigma}_{13}(z) = \frac{\sigma_{13}(0, a/2, z)}{\sigma_{13}(0, a/2, h/2)}, \qquad \bar{\sigma}_{11}(z) = \frac{\sigma_{11}(a/2, a/2, z)}{\sigma_{11}(a/2, a/2, 0)} \tag{52}$$

The accuracy of our model can be noted for a thick plate ($a/h = 4$). The continuity of the electrostatic potential, as well that of the electric displacement, is satisfied. We conclude that because our model is in very good agreement with the exact three-dimensional solution, it is efficient, because for this five-layered piezoelectric plate, it keeps only five generalized displacements and two generalized electrostatic potentials as unknowns.

B. Application of the Piezoelectric Plate Model to Statics

We consider a three-layered piezoelectric plate in the cylindrical bending configuration. The plate is supposed to be simply supported. Its lateral surfaces are subjected to electrical (closed circuit) and traction (pressure on its top face) conditions independent of the thickness coordinate. The panel is, thus, subjected to a simply sinusoidal force density on its top face:

$$p(x_1, t) = p_0 e^{j\omega t} \sin p_1 x_1 \tag{53}$$

where

$$p_1 = \pi/a \tag{54}$$

and is in closed circuit. The value of p_0 is set to 10 N/m^2. The shear stresses on the top and bottom faces are specified to be zero. The boundary conditions are

$$w(0, x_2, z, t) = w(a, x_2, z, t) = 0 \tag{55}$$

Stresses, strains, displacements, electric field, and potential do not depend on the x_2 variable. The displacement U_2 plays no role and can be canceled out. We, thus, set $u_2 = 0$ and $\gamma_2^0 = 0$. The height of the plate is fixed at $h = 0.01$ m. The plate is a 0/90/0 laminate, constituted of PVDF. (See Table 1 for the properties of PVDF.)

From Eqs. (10) and (16), the approximation of the electrostatic potential, thus, becomes

$$\begin{aligned}\varphi(x_j, t) = {} & \left\{\tfrac{1}{2}\xi^1(\xi^1 - 1)\varphi^{1B}(x_\alpha, t) + [1 - (\xi^1)^2]\varphi^{1M}(x_\alpha, t)\right. \\ & \left. + \tfrac{1}{2}\xi^1(\xi^1 + 1)\varphi^{2B}(x_\alpha, t)\right\}\chi^1 + \left\{\tfrac{1}{2}\xi^2(\xi^2 - 1)\varphi^{2B}(x_\alpha, t)\right. \\ & \left. + [1 - (\xi^2)^2]\varphi^{2M}(x_\alpha, t) + \tfrac{1}{2}\xi^2(\xi^2 + 1)\varphi^{3B}(x_\alpha, t)\right\}\chi^2 \\ & + \left\{\tfrac{1}{2}\xi^3(\xi^3 - 1)\varphi^{3B}(x_\alpha, t) + [1 - (\xi^3)^2]\varphi^{3M}(x_\alpha, t)\right. \\ & \left. + \tfrac{1}{2}\xi^3(\xi^3 + 1)\varphi^{4B}(x_\alpha, t)\right\}\chi^3 \end{aligned} \tag{56}$$

The imposed conditions are the same as in Eq. (39).

The symmetry again requires satisfying the following equations:

$$\varphi^{1M}(x_\alpha, t) = \varphi^{3M}(x_\alpha, t) \tag{57}$$

The continuity of the electric displacement is written as in Eq. (42). Hence, the electrostatic potential is obtained as earlier:

$$\varphi(x_j, t) = Q^{1M}(z)\varphi^{1M}(x_\alpha, t) + Q^{2M}(z)\varphi^{2M}(x_\alpha, t) \tag{58}$$

where Q^{1M} and Q^{2M} are functions of the thickness coordinate z, which expression is the same as in Eq. (45), with values for the constants $\lambda^{2B,1M}$ and $\lambda^{2B,2M}$ corresponding to the plate material properties.

The mechanical generalized displacements remaining unknowns are u_1, w, and γ_1^0. The electrical generalized unknowns are φ^{1M} and φ^{2M}.

The solution of Eqs. (28–33), including Eqs. (8), (25), and (44), in terms of the generalized unknowns given by Eq. (36), is sought under the form

$$\bar{u}_1(x_1, t) = A_1 e^{j\omega t}\cos p_1 x_1, \qquad \bar{w}(x_1, t) = B e^{j\omega t}\sin p_1 x_1$$
$$\bar{\gamma}_1^0(x_1, t) = C_1 e^{j\omega t}\cos p_1 x_1 \tag{59}$$

$$\bar{\varphi}^{1M}(x_\alpha, t) = \Phi_1 e^{j\omega t}\sin p_1 x_1, \qquad \bar{\varphi}^{2M}(x_\alpha, t) = \Phi_2 e^{j\omega t}\sin p_1 x_1 \tag{60}$$

where

$$p_1 = \pi/a \tag{61}$$

When these expressions are substituted into the equilibrium equations given by Eqs. (39–45) with Eqs. (20), (36), and (71), a linear system

$$K^2 X^2 = B^2 \tag{62}$$

is obtained, where

$$X^2 = (A_1, B, C_1, \Phi_1, \Phi_2) \tag{63}$$

The coefficients of K^2 and B^2 are given in Appendix B.

This system is solved using the Linear Solve procedure of Mathematica.[27]

The through-the-thickness distribution of the normalized electrostatic potential

$$\bar{\varphi}(z) = \frac{\bar{\varphi}(z)}{\varphi(h/2)} \tag{64}$$

the normalized longitudinal displacement at $x_1 = 0$

$$\bar{U}_1(z) = \frac{U_1(0, z)}{U_1(0, 0)} \tag{65}$$

the normalized shear-stress

$$\bar{\sigma}_{13}(z) = \frac{\sigma_{13}(0, z)}{\sigma_{13}(0, h/2)} \tag{66}$$

and the normalized in-plane stress

$$\bar{\sigma}_{11}(z) = \frac{\sigma_{11}(h/2, z)}{\sigma_{11}(h/2, h)} \tag{67}$$

are shown in Figs. 7–14 for $a/h = 4$ and 100. The results obtained with our model are compared to the three-dimensional solution of Heyliger and Brooks.[19]

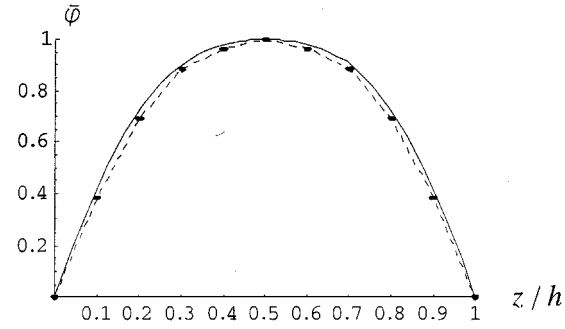

Fig. 7 Thickness distribution of the normalized electrostatic potential, three-layered plate, *a/h* = 4: ——, model and ●, exact solution.

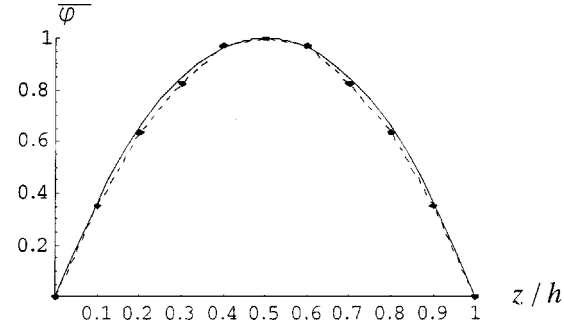

Fig. 8 Thickness distribution of the normalized electrostatic potential, three-layered plate, *a/h* = 100: ——, model and ●, exact solution.

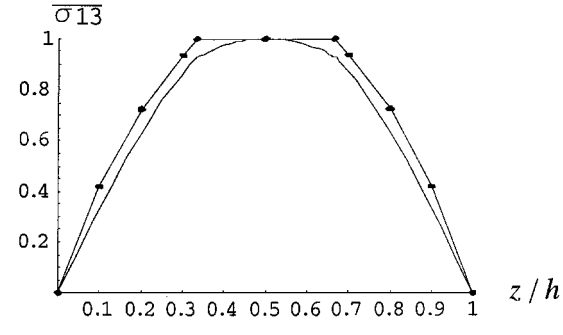

Fig. 9 Thickness distribution of the normalized shear-stress $\bar{\sigma}_{13}$, three-layered plate, *a/h* = 4: ——, model and ●, exact solution.

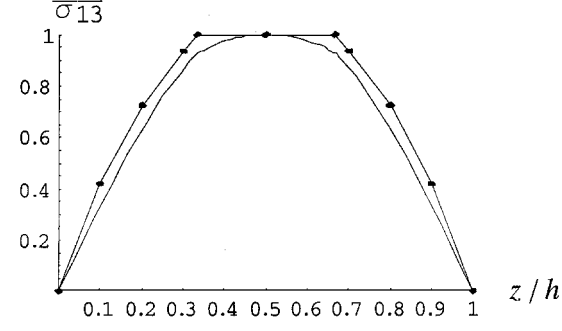

Fig. 10 Thickness distribution of the normalized shear-stress $\bar{\sigma}_{13}$, three-layered plate, *a/h* = 100: ——, model and ●, exact solution.

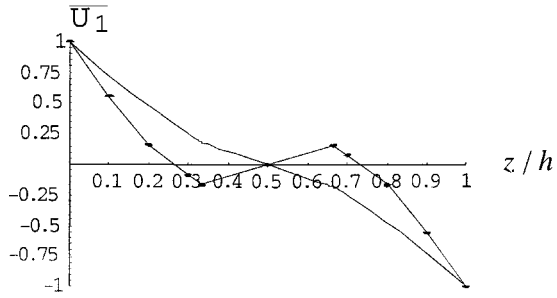

Fig. 11 Thickness distribution of the normalized displacement, three-layered plate, $a/h = 4$: ——, model and ●, exact solution.

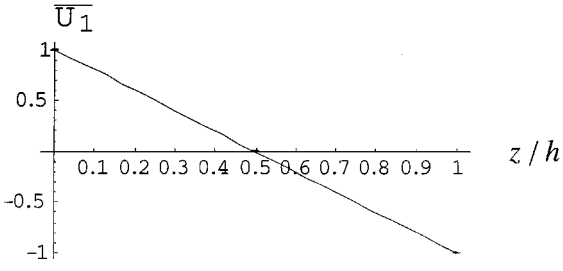

Fig. 12 Thickness distribution of the normalized displacement, three-layered plate, $a/h = 100$: ——, model and ●, exact solution.

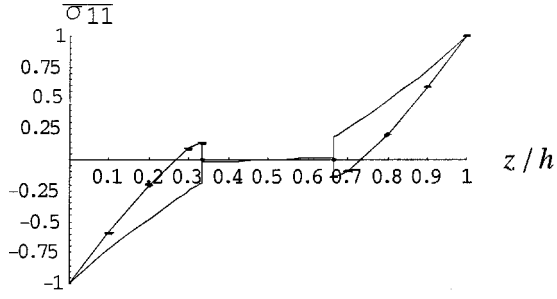

Fig. 13 Thickness distribution of the normalized in-plane stress $\bar{\sigma}_{11}$, three-layered plate, $a/h = 4$: ——, model and ●, exact solution.

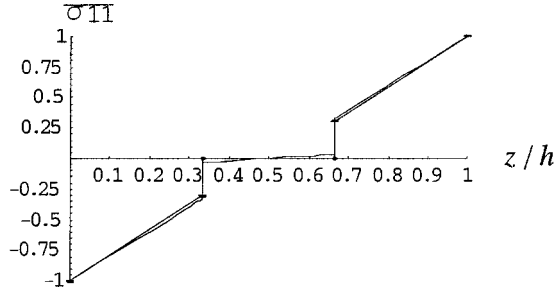

Fig. 14 Thickness distribution of the normalized in-plane stress $\bar{\sigma}_{11}$, three-layered plate, $a/h = 100$: ——, model and ●, exact solution.

Note that our model yields accurate results for the potential, even in the case of a thick plate.

For the transverse shear stress, results also appear to be accurate. The continuity at layer interfaces is not affected by the electromechanical coupling. For the longitudinal displacement and the in-plane stress, there is a noticeable difference between the thick case, $a/h = 4$, and the thin one, $a/h = 100$. The same results can be noted for purely mechanical problems.

The two cases described, and others, which do not appear here, show that our model gives accurate results for the electrostatic potential. The type of loading, electrical or mechanical, does not affect our model. The thickness of the plate, of course, affects it, yet results for mechanical quantities are in the range of what can be expected when a plate becomes thicker. The number of stacking sequences, as long as the thickness does become too high, has no effect: We have presented five-layered and three-layered plates; we also obtained excellent results for single-layered and bilayered plates. Moreover, the electromechanical coupling does not seem to affect the continuity of the transverse shear stress.

IV. Conclusions

A new refined bidimensional piezoelectric plate theory, which allows the compatibility conditions for displacements and the electrostatic potential at layer interfaces, as well as the imposed electromechanical conditions, to be satisfied is proposed. This theory also takes into account refinements of the shear and membrane terms, by means of trigonometric functions. The accuracy of the model is assessed by applying the theory to multilayered plate problems for which an exact three-dimensional solution is known.[18,19] It appears that the present model is simple to use, incorporating only five independent generalized displacements and one or two independent generalized electrostatic potential as unknowns. This is obtained from the exact satisfaction of boundary and interface conditions independently for mechanics and electricity (potential and electric displacement), which is a first within a layerwise approach. It results in reducing the number of unknowns. Then, the coupled piezoelectric model is deduced from the boundary-value problem, where we use the coupled piezoelectric law for the mechanical and electric fields satisfying all of the separately imposed conditions. This is the novelty of our approach linked to a refined multilayered plate theory. Results show that this approach is numerically consistent with prescribed interface and top and bottom conditions, when computing distributions of stresses and electric displacements throughout the thickness of the multilayered plate. Eventually, results are in very good agreement with either the exact three-dimensional solution or the three-dimensional finite element computation, but our model is probably the one that incorporates the fewest unknowns (independant generalized displacements and electrostatic potentials).

This theory will be extended to multilayered piezoelectric shells.

Appendix A: First Example

The stiffness matrix K^1 used for the example in Sec. III.A. is given by

$$K^1 = \begin{bmatrix} K^1_{11} & K^1_{12} & K^1_{13} & K^1_{14} & K^1_{15} & K^1_{16} & K^1_{17} \\ & K^1_{22} & K^1_{23} & K^1_{24} & K^1_{25} & K^1_{26} & K^1_{27} \\ & & K^1_{33} & K^1_{34} & K^1_{35} & K^1_{36} & K^1_{37} \\ & & & K^1_{44} & K^1_{45} & K^1_{46} & K^1_{47} \\ & & & & K^1_{55} & K^1_{56} & K^1_{57} \\ & & \text{sym} & & & K^1_{66} & K^1_{67} \\ & & & & & & K^1_{77} \end{bmatrix}$$

where

$$K^1_{11} = \int_0^h \left\{ p^2 C^*_{11} + \frac{1}{2} q^2 C^*_{66} \right\} \mathrm{d}z$$

$$K^1_{12} = \int_0^h \left\{ pq C^*_{12} + \frac{1}{2} pq C^*_{66} \right\} \mathrm{d}z$$

$$K^1_{13} = \int_0^h \left\{ -p\left[p^2 C^*_{11} + q^2 C^*_{12} \right] - pq^2 C^*_{66} \right\} z \, \mathrm{d}z$$

$$K^1_{14} = \int_0^h \left\{ p^2 C^*_{11} + q^2 C^*_{66} \right\} h_1(z) \, \mathrm{d}z$$

$$K^1_{15} = \int_0^h \left\{ pq C^*_{12} + pq C^*_{66} \right\} h_2(z) \, \mathrm{d}z$$

$$K_{16}^1 = -\int_0^h pe_{31}^* Q_{1M}'(z)\,\mathrm{d}z, \qquad K_{17}^1 = -\int_0^h pe_{31}^* Q_{2M}'(z)\,\mathrm{d}z$$

$$K_{22}^1 = \int_0^h \left\{q^2 C_{22}^* + p^2 C_{66}^*\right\}\mathrm{d}z$$

$$K_{23}^1 = \int_0^h \left\{-q\left[p^2 C_{12}^* + q^2 C_{22}^*\right] - qp^2 C_{66}^*\right\} z\,\mathrm{d}z$$

$$K_{24}^1 = \int_0^h \left\{pqC_{12}^* + pqC_{66}^*\right\} h_1(z)\,\mathrm{d}z$$

$$K_{25}^1 = \int_0^h \left\{q^2 C_{22}^* + p^2 C_{66}^*\right\} h_2(z)\,\mathrm{d}z$$

$$K_{26}^1 = -\int_0^h qe_{32}^* Q_{1M}'(z)\,\mathrm{d}z, \qquad K_{27}^1 = -\int_0^h qe_{32}^* Q_{2M}'(z)\,\mathrm{d}z$$

$$K_{34}^1 = \int_0^h \left\{-p^3 C_{11}^* - pq^2 C_{12}^* - pq^2 C_{66}^*\right\} z h_1(z)\,\mathrm{d}z$$

$$K_{35}^1 = \int_0^h \left\{-q^3 C_{12}^* - p^2 qC_{22}^* - p^2 qC_{66}^*\right\} z h_2(z)\,\mathrm{d}z$$

$$K_{36}^1 = \int_0^h \left\{p^2 e_{31}^* + q^2 e_{32}^*\right\} Q_{1M}'(z)\,\mathrm{d}z$$

$$K_{37}^1 = \int_0^h \left\{p^2 e_{31}^* + q^2 e_{32}^*\right\} Q_{2M}'(z)\,\mathrm{d}z$$

$$K_{44}^1 = \int_0^h \left\{\left[p^2 C_{11}^* + pqC_{66}^*\right] h_1^2(z) + \frac{1}{2} C_{55}^* h_1'^2(z)\right\}\mathrm{d}z$$

$$K_{45}^1 = \int_0^h \left\{pqC_{12}^* + pqC_{66}^*\right\} h_1(z) h_2(z)\,\mathrm{d}z$$

$$K_{46}^1 = -\int_0^h pe_{31}^* Q_{1M}'(z) h_1(z)\,\mathrm{d}z$$

$$K_{47}^1 = -\int_0^h pe_{31}^* Q_{2M}'(z) h_1(z)\,\mathrm{d}z$$

$$K_{55}^1 = \int_0^h \left\{\left[q^2 C_{22}^* + \frac{1}{2} pqC_{66}^*\right] h_2^2(z) + C_{44}^* h_2'^2(z)\right\}\mathrm{d}z$$

$$K_{56}^1 = -\int_0^h qe_{32}^* Q_{1M}'(z) h_2(z)\,\mathrm{d}z$$

$$K_{57}^1 = -\int_0^h qe_{32}^* Q_{2M}'(z) h_2(z)\,\mathrm{d}z$$

$$K_{66}^1 = -\int_0^h \left\{\left[p^2 \varepsilon_{11}^* + q^2 \varepsilon_{22}^*\right] Q_{1M}^2(z) + \varepsilon_{33}^* Q_{1M}'^2(z)\right\}\mathrm{d}z$$

$$K_{67}^1 = -\int_0^h \left\{\left[p^2 \varepsilon_{11}^* + q^2 \varepsilon_{22}^*\right] Q_{1M}(z) Q_{2M}(z) + \varepsilon_{33}^* Q_{1M}'(z) Q_{2M}'(z)\right\}\mathrm{d}z$$

$$K_{77}^1 = -\int_0^h \left\{\left[p^2 \varepsilon_{11}^* + q^2 \varepsilon_{22}^*\right] Q_{2M}^2(z) + \varepsilon_{33}^* Q_{2M}'^2(z)\right\}\mathrm{d}z$$

where Q^{1M} and Q^{2M} are given in Sec. III and coefficients K_{IJ}^1 of this matrix are computed by the numerical integration of Gauss.

The mass matrix M used in the example in Sec. III.A is given by

$$M = \begin{bmatrix} I_1 & 0 & -pI_2 & I_3^{(1)} & 0 & 0 \\ & I_1 & -qI_2 & 0 & I_3^{(2)} & 0 \\ & & I_1 + (p^2+q^2)I_4 & -pI_5^{(1)} & -qI_5^{(2)} & 0 \\ & & & I_6^{(1)} & 0 & 0 \\ & \text{sym} & & & I_6^{(2)} & 0 \\ & & & & & 0 \end{bmatrix}$$

Inertia coefficients in M, calculated from Eq. (32), are integrated numerically using the Gauss rule.

Appendix B: Second Example

The stiffness matrix available for the example in Sec. III.B is given by

$$K^2 = \begin{bmatrix} K_{11}^2 & K_{12}^2 & K_{13}^2 & K_{14}^2 & K_{15}^2 \\ & K_{22}^2 & K_{23}^2 & K_{24}^2 & K_{25}^2 \\ & & K_{33}^2 & K_{34}^2 & K_{35}^2 \\ & \text{sym} & & K_{44}^2 & K_{45}^2 \\ & & & & K_{55}^2 \end{bmatrix}$$

The coefficients K_{IJ}^2 are computed from the following expressions, using a numerical integration rule of Gauss to perform integrals:

$$K_{11}^2 = \int_0^h p^2 C_{11}^*\,\mathrm{d}z, \qquad K_{12}^2 = -\int_0^h p^3 C_{11}^* z\,\mathrm{d}z$$

$$K_{13}^2 = \int_0^h p^2 C_{11}^* h_1(z)\,\mathrm{d}z, \qquad K_{14}^2 = -\int_0^h pe_{31}^* Q^{1M'}(z)\,\mathrm{d}z$$

$$K_{15}^2 = -\int_0^h pe_{31}^* Q^{2M'}(z)\,\mathrm{d}z, \qquad K_{22}^2 = \int_0^h p^4 C_{11}^* z^2\,\mathrm{d}z$$

$$K_{23}^2 = -\int_0^h p^3 C_{11}^* z h_1(z)\,\mathrm{d}z, \qquad K_{24}^2 = \int_0^h p^2 e_{31}^* Q^{1M'}(z)\,\mathrm{d}z$$

$$K_{25}^2 = \int_0^h p^2 e_{31}^* Q^{2M'}(z)\,\mathrm{d}z$$

$$K_{33}^2 = \int_0^h \left\{p^2 C_{11}^* h_1^2(z) + C_{55}^* h_1'^2(z)\right\}\mathrm{d}z$$

$$K_{34}^2 = -\int_0^h pe_{31}^* Q^{1M'}(z) h_1(z)\,\mathrm{d}z$$

$$K_{35}^2 = -\int_0^h pe_{31}^* Q^{2M'}(z) h_1(z)\,\mathrm{d}z$$

$$K_{44}^2 = -\int_0^h \left\{p^2 \varepsilon_{11}^* Q^{1M^2}(z) + \varepsilon_{33}^* Q^{1M'^2}(z)\right\}\mathrm{d}z$$

$$K_{45}^2 = -\int_0^h \left\{p^2 \varepsilon_{11}^* Q^{2M^2}(z) + \varepsilon_{33}^* Q^{2M'^2}(z)\right\}\mathrm{d}z$$

$$K_{55}^2 = -\int_0^h \left\{p^2 \varepsilon_{11}^* Q^{2M^2}(z) + \varepsilon_{33}^* Q^{2M'^2}(z)\right\}\mathrm{d}z$$

Vector $\boldsymbol{B}$ is

$$\boldsymbol{B}^0 = \begin{bmatrix} 0 \\ -p_0 \\ 0 \\ 0 \\ 0 \end{bmatrix}$$

References

[1]Tiersten, H.-F., *Linear Piezoelectric Plate Vibrations*, Plenum, New York, 1969.

[2]Mindlin, R. D., "High Frequency Vibrations of Piezoelectric Crystal Plates," *International Journal of Solids and Structures*, Vol. 8, 1972, pp. 895–906.

[3]Lee, C. K., and Moon, F. C., "Laminated Piezopolymer Plates for Torsion and Bending Sensors and Actuators," *Journal of the Acoustical Society of America*, Vol. 85, No. 6, 1989, pp. 2432–2439.

[4]Lee, C. K., "Theory of Laminated Piezoelectric Plates for the Design of Distributed Sensors/Actuators. Part 1: Governing Equations and Reciproqual Relationship," *Journal of the Acoustical Society of America*, Vol. 87, No. 3, 1990, pp. 1144–1158.

[5]Chandrashekhara, K., and Agarwal, A. N., "Active Vibration Control of Laminated Composite Plates Using Piezoelectric Devices: A Finite Element Approach," *Journal of Intelligent Materials Systems and Structures*, Vol. 4, No. 4, 1993, pp. 496–508.

[6]Tauchert, T. R., "Piezothermoelastic Behavior of a Laminated Plate," *Journal of Thermal Stresses*, Vol. 15, No. 1, 1992, pp. 25–37.

[7]Vatal'yan, A. O., Getman, I. P., and Lapitskaia, N. B., "Flexure of a Piezoelectric Bimorph Plate," *Prikladnaya Matematikay Mekanika*, Vol. 27, No. 10, 1992, pp. 101–105.

[8]Lee, P. C. Y., Syngellakis, S., and Hou, J. P., "A Two-Dimensional Theory for High Frequency Vibrations of Piezoelectric Crystal Plates with or Without Electrodes," *Journal of Applied Physics*, Vol. 61, 1987, pp. 1249–1262.

[9]Yang, J. S., and Yu, J. D., "Equations for a Laminated Piezoelectric Plate," *Archives of Mechanics*, Vol. 45, 1993, p. 653.

[10]Yong, Y. K., Stewart, J. T., and Ballato, A., "A Laminated Plate Theory for High Frequency, Piezoelectric Thin-Film Resonators," *Journal of Applied Physics*, Vol. 74, No. 5, 1993, pp. 3028–3046.

[11]Zhang, X. D., and Sun, C. T., "Formulation of an Adaptative Sandwich Beam," *Smart Material Structures*, Vol. 5, 1996, pp. 814–823.

[12]Mitchell, J. A., and Reddy, J. N., "A Refined Hybrid Plate Theory for Composite Laminates with Piezoelectric Laminae," *International Journal of Solids and Structures*, Vol. 32, No. 16, 1995, pp. 2345–2367.

[13]Fernandes, A., "Modèle et Étude de Composants Piézoélectriques: Applications aux Structures Multifonctionnelles," Ph.D. Dissertation, Laboratoire de Modélisation en Mécanique, Univ. Paris VI, Paris, 2000.

[14]Fernandes, A., and Pouget, J., "Two-Dimensional Modelling of Laminated Piezoelectric Composites: Analysis and Numerical Results," *Journal of Thin-Walled Structures*, Vol. 39, No. 1, 2001, pp. 3–22.

[15]Touratier, M., "An Efficient Standard Plate Theory," *International Journal of Engineering Science*, Vol. 29, No. 8, 1991, pp. 901–916.

[16]Pauley, K. E., "Analysis of Plane Waves in Infinite Laminated, Piezoelectric Plates," Ph.D. Dissertation, Dept. of Engineering, Univ. of California, Los Angeles, 1974.

[17]Pai, P. F., Nayfeh, A. H., Oh, K. Y., and Mook, D. T., "A Refined Nonlinear Model of Composite Plates with Integrated Piezoelectric Actuators and Sensors," *International Journal of Solids and Structures*, Vol. 30, No. 12, 1993, pp. 1603–1630.

[18]Heyliger, P., "Exact Free-Vibration Analysis of Laminated Plates with Embedded Piezoelectric Layers," *Journal of the Acoustical Society of America*, Vol. 98, No. 3, 1995, pp. 1547–1557.

[19]Heyliger, P., and Brooks, S., "Exact Solutions for Laminated Piezoelectric Plates in Cylindrical Bending," *Journal of Applied Mechanics*, Vol. 63, No. 3, 1996, pp. 903–910.

[20]Cheng, Z.-Q., and Batra, R. C., "Three-Dimensional Analysis of Multiple-Electroded Piezoelectric Laminates," *AIAA Journal*, Vol. 38, No. 2, 2000, pp. 317–324.

[21]Ossadzow, C., Muller, P., and Touratier, M., "Wave Dispersion in Deep Multilayered Doubly Curved Viscoelastic Shells," *Journal of Sound and Vibration*, Vol. 214, No. 3, 1998, pp. 531–552.

[22]Ossadzow, C., Touratier, M., and Muller, P., "Deep Doubly Curved Multilayered Shell Theory," *AIAA Journal*, Vol. 37, No. 1, 1999, pp. 100–109.

[23]Touratier, M., "A Refined Theory of Laminated Shallow Shells," *International Journal of Solids and Structures*, Vol. 29, No. 11, 1992, pp. 1401–1415.

[24]Di Sciuva, M., "An Improved Third-Order Shear Deformation Theory for Moderately Thick Multilayered Anisotropic Shells and Plates," *Journal of Applied Mechanics*, Vol. 54, 1987, pp. 589–596.

[25]He, L.-H., "A Linear Theory of Laminated Shells Accounting for Continuity of Displacements and Transverse Shear Stresses at Layer Interfaces," *International Journal of Solids and Structures*, Vol. 31, No. 5, 1994, pp. 613–627.

[26]Cheng, S., "Elasticity Theory of Plates and a Refined Theory," *Journal of Applied Mechanics*, Vol. 46, No. 3, 1979, pp. 644–650.

[27]Wolfram, S., *The Mathematica Book*, Ver. 4, 4th ed., Cambridge Univ. Press, Cambridge, England, U.K., 1999, pp. 880, 881, 1062, 1180.

M. Ahmadian
Associate Editor